Developmental regulation and evolution of cAMP signalling in Dictyostelium

Alvarez-Curto, E.

Chapter Five

Evolutionary origins of cAMP signalling in the social amoebas

A revised form of this Chapter was published in *Proc. Natl. Acad. Sci. USA*, 2005; 102, 6385-6390
Evolutionary origin of cAMP-based chemoattraction in the social amoebae
Elisa Alvarez-Curto, Daniel E. Rozen, Alysson V. Ritchie, Celine Fouquet, Sandra L. Baldauf, and Pauline Schaap

Abstract

Phenotypic novelties can arise if integrated developmental pathways are expressed at new developmental stages and are then recruited to serve new functions. I have analysed the origins of a novel developmental trait of Dictyostelid amoebas: the evolution of cAMP as a developmental chemoattractant. I show in this Chapter that cAMP's role to attract starving amoebas arose through recruitment of a pathway that originally evolved to coordinate fruiting body morphogenesis. cAMP receptors (*cARs*) from basal species are only expressed during fruiting body formation, but can fully rescue cAR deletions in derived species. Abrogation of cAR function blocks all development in derived species, but only fruiting body formation in basal species. This indicates that aggregation by cAMP signalling arose through co-option of a pre-existing pathway that originally evolved to coordinate morphogenesis.

Introduction

The origin of species diversity is the story of the origin of novel features. These can arise through the development of entirely new genes (1), or when pathways underlying existing functions are co-opted to perform new ones through altered regulation of the component genes. Novel features of development, which can cause dramatic shifts in species form, are particularly thought to arise by this manner (2-4). However, few data exist to support this common view, and even fewer to document the steps involved at high phylogenetic and biochemical resolution. Here I report on the analysis of the derived origin of a novel, even group-defining, feature of Dictyostelid social amoebas: the origin of cAMP based chemoattraction.

The Dictyostelid amoebas are a diverse group of organisms that display conditional multicellularity with a range of phenotypes (5). In the model system *Dictyostelium discoideum* extracellular cAMP pulses coordinate the aggregation of starving amoebas (6). cAMP has also been implicated as a morphogen that directs subsequent fruiting body formation (7). cAMP is produced by an adenylyl cyclase, ACA, and degraded by an extracellular phosphodiesterase, PdsA (8,9). Together with cAR1 or cAR3, two of the four *D.discoideum* cAMP receptors, these enzymes are essential for oscillatory cAMP signalling (10,11).

Material and methods

Cell lines and culture

D.minutum 71-2, *D.fasciculatum* SH3, *P.pallidum* TNS-C-98 and *D.rosarium* M45 cells were grown in association with *Klebsiella aerogenes* on LP agar (5). *D.discoideum* DH1 cells were grown in HL5 medium (13). For developmental time courses, cells were harvested while in exponential phase and incubated at 22°C and 8 x 10^5 cells/cm^2 on non-nutrient agar (1.5% agar in 10 mM phosphate buffer, pH 6.5).

Gene identification

The degenerate oligonucleotides, 5'-GGTAGTTTCGCATGYTGGYTNTGGAC-3' and 5'-TCACCGAAGTATCGCCACATNTRNGGRTT-3' designed to match amino-acid sequences GSFACWLWT and NPLMWRYFG that are conserved between cARs 1-4 of *D.discoideum* were used to amplify putative cAR genes by touch-down PCR (14) from genomic DNAs of the four test species. The touch-down protocol started with 4 cycles with annealing at 60°C for 30s, 10 cycles with an annealing temperature decrement of 1°C and 20 cycles with annealing at 50°C. The PCR products were subcloned in the pGEM-T Easy vector (Promega, Madison, USA) and their sequence was determined from at least three independent clones. The *DmcAR* PCR product was used to screen a λZapII library of sheared *D.minutum* gDNA, which was custom-made by Stratagene (La Jolla, USA) from *D.minutum 71-2* gDNA provided by us. Three positive plaques, C2, C6 and C10, were identified and their pBluescript phagemids were

isolated by *in vitro* excision according to the manufacturer's instructions. The respective 3.5, 4.7 and 1.25 kb inserts were sequenced to four-fold coverage by primer walking. The sequences could be assembled into a 4873 bp contig, which apart from the *DmcAR*, contained two other ORFs. BLAST searches of the entire Genbank database showed that one partial ORF was most similar to *D.discoideum SpkA* (15), and the other complete ORF to the putative *D.discoideum* protein *DDB0217155* (http://dictybase.org/). The *D.minutum* protein was called DtmA for its only structural feature of Dual TransMembrane helices.

RNA isolation and analysis

Total RNA was isolated from 2 x 10^7 cells, size-fractionated in 1.5 % agarose gels containing 2.2 M formaldehyde and transferred to nylon membranes (16). Cells in the culmination stages were vortexed for 5 min with glass beads during RNA extraction to break stalk cells and spores. Membranes were hybridised at 65°C to [^{32}P]dATP-labelled DNA probes and washed at high stringeny according to standard procedures (17). Three microlitres of 0.28- to 6.6-kb RNA markers (Promega, UK) were run on the same gel and stained with ethidium bromide to estimate the size of the *cAR* mRNAs.

Heterologous expression of DmcAR

A 1525 bp fragment was amplified from λZAPII clone C6 using oligonucleotides that will generate BglII restriction sites (5'-CCAGATCTAAAATGGAACAATCACCCGATG-3' and 5'-CCAGATCTCAACCCCAAAACCAACAAC-3'). This fragment includes the complete 1173 bp coding region of DmcAR with 3 bp of 5'UTR and 364 bp of 3'UTR. The BglII digested product was subcloned into the BglII site of vector PJK1 (10), which placed *DmcAR* downstream of the *D.discoideum* actin15 promoter and yielded vector A15:DmcAR. The integrity of the A15:DmcAR fusion was verified by DNA sequencing. The *car1car3* mutant (18) was transformed with either A15:DmcAR or A15:DdcAR1 in PJK1 (19) and selected for growth at 20 µg/ml G418 (Sigma, USA).

cAMP binding assay

To measure cell surface cAMP binding activity, 1.6 x 10^7 cells were incubated for 1 min at 0°C with 1 or 10 nM ^{3}HcAMP (Amersham, Little Chalfont, UK), 5 mM dithiothreitol (Sigma, USA) and variable concentrations of cAMP in a total volume of 100 µl. Cells were separated from unbound ^{3}HcAMP by centrifugation for 10 s at 16,000 x g through a 4:11 mix of AR200:AR20 silicon oil (Wacker-Chemie, Burghausen, Germany). The ^{3}HcAMP associated with the cell pellet was measured by liquid scintillation counting.

Video microscopy and image analysis

An Axiovert 135 microscope (Zeiss; objectives: FLUAR 10´/NA 0.5, Plan NEOFLUAR 10´/NA 0.3) equipped with a cooled CCD camera (Hamamatsu, C4880-82) was used to record wave propagation in aggregating cells and darkfield waves during development (20,21). Images were saved as TIFFs and transferred to a PC for analysis with the Optimas software (MediaCybernetics, version 6.1). Standard image processing techniques like image subtraction were applied to improve the visibility of the optical density waves. To determine wave propagation speed and periodicity time-space-plots were generated and analysed as described previously (20,21).

Phylogenetic analysis

For the cAR protein tree, sequences were aligned with ClustalX (22) using default parameters. Only ungapped regions (or with small gaps in single sequences) and flanked by 70% consensus sites were used. The tree shown was derived by maximum likelihood and

Bayesian Inference analyses on 291 unambiguously aligned amino acid positions. The Bayesian inference utilised MrBayes V3.0 (23) with posterior probabilities (biPP) values estimated from 10^7 chains and discarding a burnin of 1000. Maximum likelihood bootstrap percentage (mlBP) values were determined from 500 replicates using the PROML program from the PHYLIP package (24). Both analyses utilized the JTT model (25) for weighting amino acid substitutions and a gamma correction for rate variation among sites. An α value of 1.39 was used for the gamma distribution in the mlBP analyses, as determined by the program Tree-Puzzle (26). Support values for the *cAR*+*TasA* subtree were determined from a dataset consisting of only these nine sequences, to avoid loss of resolution due to long-branch attraction to the distantly related outgroup sequences. The full dataset of 13 sequences was then used to test the deeper nodes. Four G-protein coupled receptor (GPCR) sequences were used to root the tree as these were shown to be the most conservative (relative to the cAR sequences) based on phylogenetic analyses using a range of cAR-related sequences.

For the small subunit ribosomal RNA (SSU rDNA) tree, complementary DNA sequences were aligned by eye and only unambiguously aligned, ungapped regions were used to construct the tree. Both Bayesian Inference and maximum likelihood analyses utilised the general-time-reversible model with a gamma correction for rate variation among sites and a designated proportion of invariant sites (GTR+I+G). The biPP values were estimated from 10^7 chains with a burnin of 10000 and mlBP values from 100 replicates. All parameters were estimated from the data by the respective phylogenetic programs.

Results

Identification of cAR-like sequences in four Dictyostelid species

As shown in the phylogeny of Chapter Four, the Dictyostelids can be subdivided into 4 major groups. *D.discoideum (Dd)* lies within the most derived Group 4, which is nested within a series of three progressively deeper lineages, the most basal of which is Group 1, the taxon closest to the outgroup of solitary amoebas (27). We selected four taxa, *D.fasciculatum (Df)*, *P.pallidum (Pp)*, *D.minutum (Dm)* and *D.rosarium (Dr)* for study as representatives of Groups 1,2,3 and 4 respectively (Fig. 1A). Similar to *D.discoideum* and other investigated group 4 taxa, *D.rosarium* uses cAMP as attractant. However, none of the other taxa do: *D.minutum* uses folate, *P.pallidum* glorin, and *D.fasciculatum* an unknown compound to aggregate (5, 12).

Degenerate oligonucleotide primers were designed to match amino acid sequences that are conserved between the four homologous *D. discoideum (Dd*) cARs 1–4. These primers were used to amplify cAR-like sequences by touch-down PCR from genomic DNAs of the four test species, *D. fasciculatum*, *P.pallidum*, *D. minutum*, and *D. rosarium.* Single cAR-like sequences were obtained from *D. fasciculatum* (*DfcAR*), *P. pallidum* (*PpcAR*), and *D. minutum* (*DmcAR*) and dual sequences from *D. rosarium* (*DrcARI* and *DrcARII*). The sequences varied in size due to a variable-length intron, present in all sequences except in *DmcAR*. These introns were located at the same conserved position as the single intron in *D. discoideum* cAR1–4. The derived amino acid sequences of the *cAR* genes showed 71–87% identity with DdcAR1 (Fig. 1*A*). *PpcAR* was identical to *TasA*, a putative receptor from *P. pallidum* (28). Phylogenetic analysis showed that *DfcAR, DmcAR, PpcAR, DrcARI*, and *DdcAR1* represent the ancestral cAR receptor lineage from which *cAR2–4* were derived, including *DrcARII*, which is specifically related to *DdcAR2* (Fig. 1*B*). The cAR phylogeny closely mirrors the small subunit RNA phylogeny of the five species (Fig. 1*C*) (27), albeit that in both trees, the nodes that define the relative positions of *P. pallidum* and *D. fasciculatum* are less well resolved than the other nodes.

Developmental regulation of *cAR* expression

We assessed the developmental role of the putative *cARs* by comparing their expression during the life cycles of the five taxa. A *D.discoideum* developmental time course was included for comparison. In the most basal taxa *D.fasciculatum* and *P.pallidum*, a single

cAR mRNA appears after aggregation is completed, and this mRNA remains present until fruiting bodies are formed (Fig. 2).

D.minutum expresses two *cAR* transcripts, a smaller mRNA that occurs during growth and then decreases, and a larger mRNA that appears once tight aggregates have formed. *D.rosarium* (*DrcARI)* also yields two different size transcripts, but here, as for its close relative *DdcAR1* (29, 30), the smaller mRNA species appears just before aggregation, while a larger species appears after aggregation is completed.

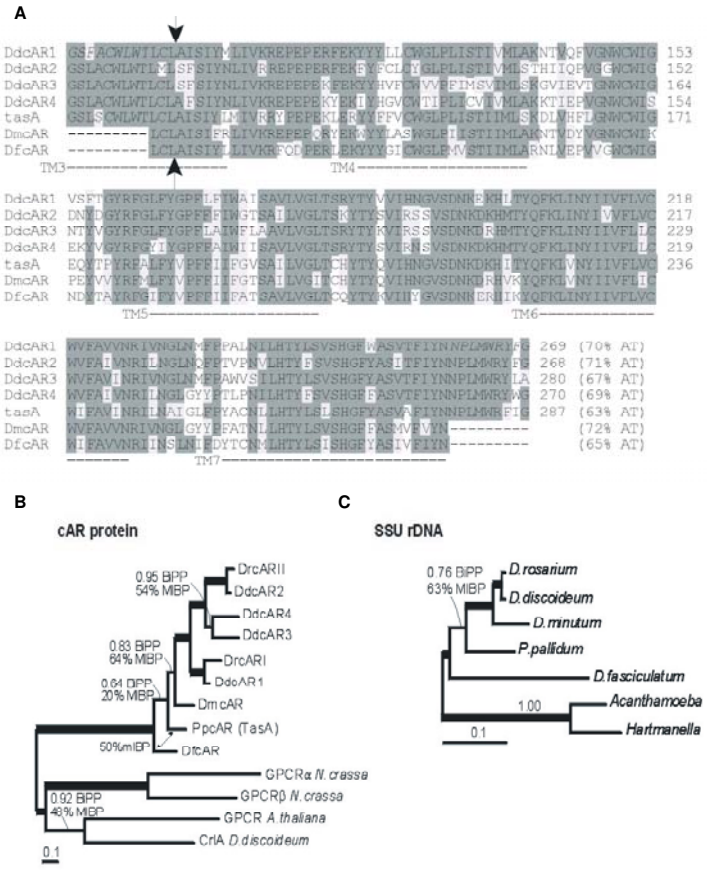

Figure 1. Identifation of cAR-like sequences in four Dictyostelid species. (*A*) Alignment of cAR-like sequences from four test species with the *D. discoideum cARs*. DNA fragments of 543–627 bp were amplified from *D. fasciculatum*, *D.minutum*, *P. pallidum*, and *D.rosarium* genomic DNA by using degenerate oligonucleotides that match conserved sequences in the four *D. discoideum* cARs. After excision of a variable length intron at a conserved position (arrows), the derived amino acid sequences were determined and aligned by using CLUSTAL-X. Amino acid residues that are identical in the majority or at least four of the nine sequences are shaded grey. The conserved regions used for oligonucleotide design are shown for *DdcAR1–4*, for *PpcAR*, which is identical to *TasA* (28), and for *DmcAR*. The positions of the putative transmembrane (TM) domains 3–7 of *DdcAR1* (35) are indicated. GenBank accession nos: A41238 (*DdcAR1*), A46390 (*DdcAR2*), A46391 (*DdcAR3*), A54813 (*DdcAR4*), and AB045712 (*TasA*). (*B*) Phylogenetic analysis of cAR-like sequences. The tree shown was derived by maximum likelihood analysis (mIBP) and Bayesian inference (BiPP) and is drawn to scale, as indicated by the scale bar (0.1 substitutions per site). Thick lines indicate nodes with 1.00 Bayesian inference posterior probabilities and 100% mIBP support. An alternative branching pattern among the two deepest cAR nodes favored by mIBP is indicated by a double-headed arrow. Four putative G protein-coupled receptor sequences were used to root the tree. *N. crassa*. *Neurospora crassa*. GenBank accession nos.: AAM20722 (*AtGPCR*), AAO62367 (*DdcrlA*), EAA35706 (*NcGPCRα*), and EAA28751 (*NcGPCRβ*). (*C*) Molecular phylogeny of Dictyostelids based on small subunit rDNA sequences. The tree shown was derived by using Bayesian inference and maximum likelihood analysis on 1,556 unambiguously aligned nucleotide positions. Sequences from solitary amoebas were used to root the tree.

As is the case for the more basal Dictyostelids, the post-aggregative mRNA remains present until development is completed. In case of *DrcAR1* the smaller mRNA species also persists. Because both hybridization and washing of the Northern blots were performed at high stringency, the additional bands are unlikely to result from nonspecific hybridization to other cAR genes. Expression of two mRNA species from a single gene was previously demonstrated for *DdcAR1* (30). The *cAR* mRNAs varied between 1.4 and 2.1 kb in size; however, even the smallest 1.4-kb mRNA of *D. minutum* is large enough to accommodate the complete

1.16-kb *DmcAR* coding region. We could not detect any mRNA hybridizing to the *DrcARII* probe, which indicates that this gene is expressed only at very low levels, if at all. To conclude, it appears that in the course of Dictyostelid evolution, the expression of a single *cAR1*-type mRNA during culmination became supplemented with expression of a second mRNA from the same gene during pre-aggregative development.

Functional Analysis of the D. minutum cAR

The expression of *cAR1* during *D. discoideum and D. rosarium* aggregation is fully concordant with the fact that these species use cAMP to aggregate. However, the expression of a *cAR1*-like gene during *D. minutum* aggregation is enigmatic in view of the fact that *D.minutum* cells use folate and not cAMP for aggregation (31).

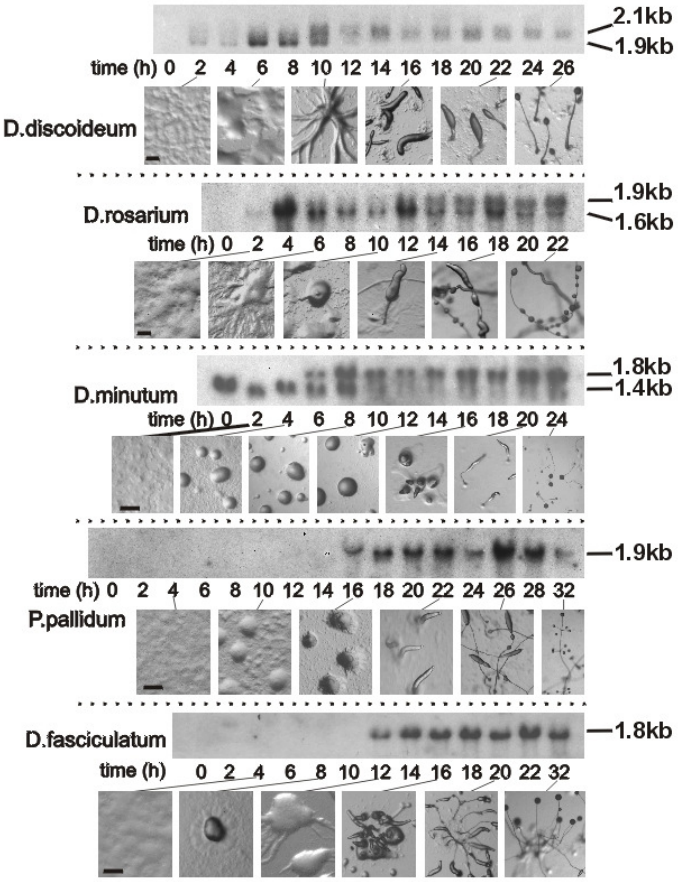

Figure 2. Developmental regulation of *cAR* gene expression Cells of the indicated five species were incubated on nonnutrient agar until fruiting bodies had formed. Total RNA was extracted at 2 hours intervals, and the progression of development was photographed. Northern blots were probed at 65°C with [^{32}P]dATP-labeled *DdcAR1* cDNA or with the [^{32}P]dATP-labeled *DrcARI*, *DmcAR*, PpcAR, and *DfcAR* PCR products, respectively, and washed at high stringency. Bar, 200 μm.

It is therefore particularly important to establish for this species that its cAR-like gene encodes a functional cAR. To do so, we cloned the full-length *DmcAR* gene from a *D. minutum* genomic DNA library and expressed it in the *D. discoideum car1car3* mutant for assay of cAMP-binding activity and functional complementation. The library screen yielded three overlapping clones, which could be assembled into a 4,873-bp contig (Fig. 3*A*). In addition to the complete 1.16-kb *DmcAR* coding sequence, this contig also contained a complete second gene, which was named *DmDtmA*, and a gene fragment, which was named *DmSpkA*. BLAST searches of the entire GenBank protein database with these sequences identified the *D. discoideum* genes *DdSpkA* and *DDB02170155* as their most related orthologues. The *D. discoideum* genes occupy the same position relative to *DdcAR1* as their *D. minutum* orthologues to *DmcAR*. The flanking genes of *DdcAR2*, *DdcAR3*, and *DdcAR4* bear no similarity to the DmcAR flanking genes. This indicates that *DmcAR* is a true orthologue of

DdcAR1, and that there is at least partial synteny between the *D. discoideum* and *D. minutum* genomes.

To determine whether the putative cARs encode functional cAMP receptors, we cloned the full-length DmcAR gene from a genomic library (Fig. 3A) and used it to complement the *D.discoideum car1car3* mutant (18). This mutant lacks high affinity receptors due to lesions in both its *cAR1* and *cAR3* genes and can consequently neither aggregate nor form fruiting bodies. We fused the DmcAR coding sequence to the constitutive *D.discoideum* A15 promoter and transformed *car1car3* with the A15:DmcAR gene fusion. *car1car3* transformed with A15:DdcAR1 was used as a control. Figure 3B shows that cells transformed with A15:DmcAR or A15:DdcAR1 bound significant amounts of ^{3}HcAMP, whereas the host *car1car3* strain bound none at all. Competition curves and Scatchard plots of ^{3}HcAMP binding (Fig. 3C) show that DdcAR1 and DmcAR give rise to both high (K_D~30 nM) and low (K_D~1 µM) affinity binding sites as reported for cAR1 in wild-type *D.discoideum* cells (32).

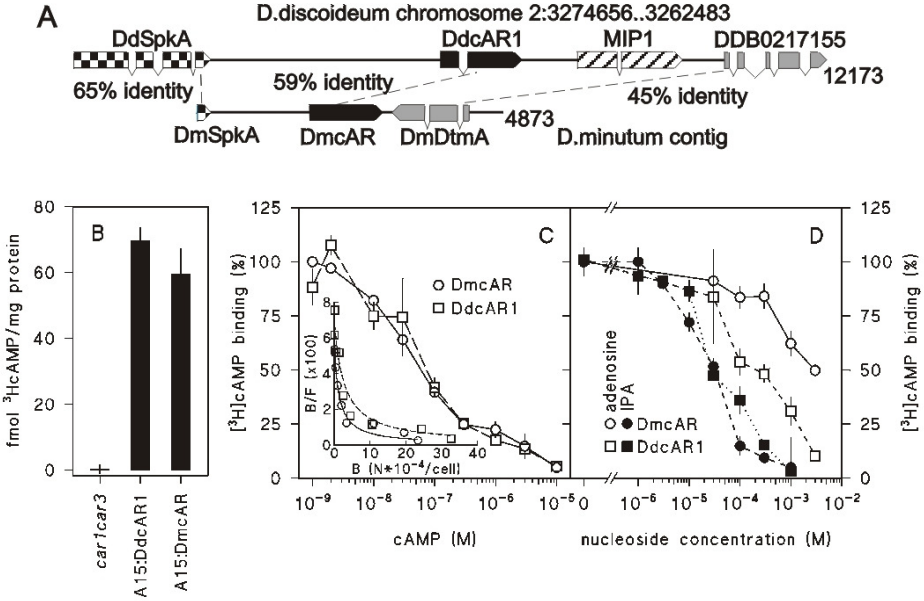

Figure 3. Cloning and cAMP-binding properties of DmcAR (*A*) Cloning of DmcAR. Screening of a *D. minutum* genomic DNA library with the *DmcAR*PCR product yielded a 4.87-kb contig of three clones. This contig contains *DmcAR* and two flanking genes, which we denote *DmSpkA* and *DmDtmA*. These genes are most similar to the *D. discoideum* genes *SpkA* and *DDB0217155*, respectively, which occupy the same positions relative to *DdcAR1* on chromosome 2 (39). The percentages of amino acid identity between the orthologous genes are indicated. (*B*) cAMP binding. *car1car3* cells, transformed with either *A15:DmcAR*, *A15:DdcAR1*, or no construct, were incubated with 10 nM [^{3}H]cAMP and assayed for cell-surface-associated [^{3}H]cAMP-binding activity. (*C*) Competition curve for cAMP. *A15:DmcAR*- or *A15:DdcAR1*-transformed *car1car3* cells were incubated with 1 nM [^{3}H]cAMP and the indicated concentrations of cAMP and assayed for [^{3}H]cAMP binding to the cell surface. The data are presented as percentage of [^{3}H]cAMP binding in the absence of cAMP and as a *Scatchard* plot (38) (*Inset*). B, bound; F, free cAMP; N, number of molecules. (*D*) Inhibition of [^{3}H]cAMP binding by adenosine and 2_3_isopropylidene adenosine (IPA).The transformed cell lines were incubated with10 nM [^{3}H]cAMP and the indicated concentrations of adenosine and IPA and assayed for [^{3}H]cAMP binding to the cell surface. The data are presented as percentage of [^{3}H]cAMP binding in the absence of nucleosides. All data represent the means and SEM of two experiments performed in triplicate.

The binding of cAMP to DdcAR1, but not to any of the other *D. discoideum* cARs, is inhibited by adenosine and more potently by the adenosine analog 2_3_isopropylidene adenosine (IPA) (19,33). We investigated whether this was also the case for the DmcAR. Fig. 3*D* shows that both adenosine and IPA inhibit ^{3}HcAMP binding to DmcAR, although inhibition by adenosine occurs less effectively for DmcAR than for DdcAR1. In conclusion, these data show that the cAMP-binding properties of DmcAR are much more similar to those of DdcAR1 than to any of the other *D. discoideum* cARs. This confirms the genetic evidence that *DmcAR* is a *DdcAR1* orthologue.

Binding of cAMP is not the sole function of cAR1, as full functionality requires DmcAR to interact with other components of the cAMP signalling system. We assessed this by compa-

ring development in the A15:DmcAR cells to the *car1car3* mutant and its parent DH1. Figure 4A shows that transformation with A15:DmcAR fully restored aggregation and fruiting body formation in *car1car3*. During aggregation of *D.discoideum* cells, cAMP pulses are propagated in complex spiral wave patterns (20,21,26,34). To investigate whether DmcAR can mediate similar complex behaviour, we tracked the optical density waves that are diagnostic for pulsatile cAMP signalling during aggregation of *car1car3*/A15:DmcAR cells. The time-lapse movie presented in figure 4B shows spiral waves propagating from an aggregation center into a field of cells, which causes the cells to move towards the center. This indicates that DmcAR fully supports pulsatile cAMP signalling in *D.discoideum*, and thus couples to downstream components of the cAMP signalling machinery. Together with the biochemical data presented above, we therefore conclude that DmcAR is a functional high affinity cAMP receptor.

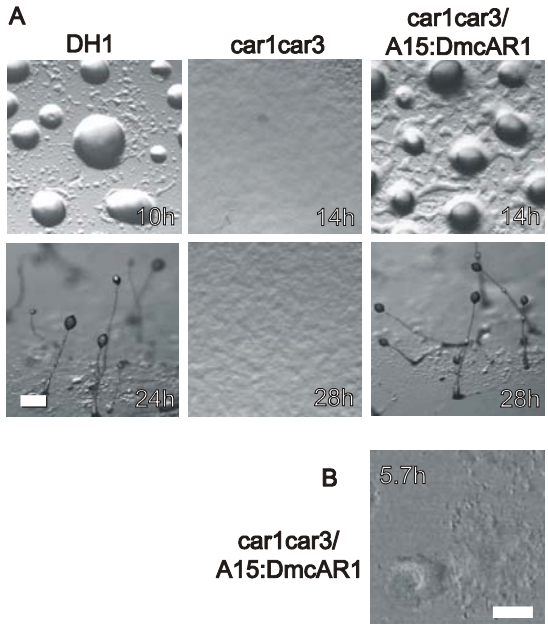

Figure 4. Complementation of *D.discoideum car1car3* by *DmcAR* (*A*) Restoration of development. The *D.discoideum car1car3* mutant, its parent strain DH1, and *car1car3* transformed with *A15:DmcAR* were incubated on non-nutrient agar at 22°C and photographed at 2-h intervals. Bar, 100 µm. (*B*) Oscillatory signaling. *car1car3_A15:DmcAR* cells were incubated for 5h at 4 x 10^5 cells per cm^2 on agar and subsequently tracked during 50 min at 10-s intervals by time-lapse video-microscopy under phase-contrast illumination. Optical density waves were enhanced by image subtraction (30). The 256th video frame is shown. Bar, 100 µm.

The Role of cARs in Basal Dictyostelid Species

Similar to all investigated group 4 taxa, *D.rosarium* uses cAMP as chemoattractant, but this is not the case for *D.fasciculatum*, *P.pallidum* and *D.minutum* (5,12). What, then, is the function of cARs in these taxa? *cAR1*-mediated signalling adapts to sustained stimulation with cAMP or its non-degradable analog SpcAMPS; this feature enables cAR1 function to be pharmacologically abrogated by exposure to excess ligand (35,36). Consistent with the known role of cAMP during *D. discoideum* aggregation, development on SpcAMPS inhibits aggregation of *D.discoideum* cells, mimicking the phenotype of *car1car3* cells. SpcAMPS can thus be used to specifically determine which aspects of development (aggregation, fruiting body formation, or both) are regulated by cAMP signalling.

Figure 5 shows that the development of all species is curtailed by SpcAMPS, although the manner in which this occurs differed among taxa. The most basal species, *D .fasciculatum*, aggregated normally with inflowing streams of cells when developing on agar containing SpcAMPS. However, while control aggregates rapidly developed into several robust upright culminants, the aggregates on SpcAMPS agar remained spread out and formed only small and aberrant structures. Similarly, in neither *P.pallidum* nor *D.minutum* was the aggregation process itself affected by SpcAMPS. In *D.minutum*, the aggregates failed to form tips, and thereafter dispersed. *P.pallidum* showed an interesting dose-dependency for the effects of SpcAMPS. At 10 µM, fruiting bodies were formed, but these had lost the whorls of side-branches that characterise this taxon. This phenotype was also reported for the *PpcAR* (*TasA*) null mutant (28). At 300 µM, tip formation on mounds was delayed and fruiting structures became very abnormal. In both *D.discoideum* and *D.rosarium*, SpcAMPS blocked the

aggregation process, consistent with the fact that both species use cAMP to aggregate. These experiments show that the basal species, *D.fasciculatum, P.pallidum and D.minutum* only require dynamic cAMP signalling during fruiting body formation. This is in contrast to the more derived species *D.discoideum* and *D.rosarium,* which also use cAMP for aggregation.

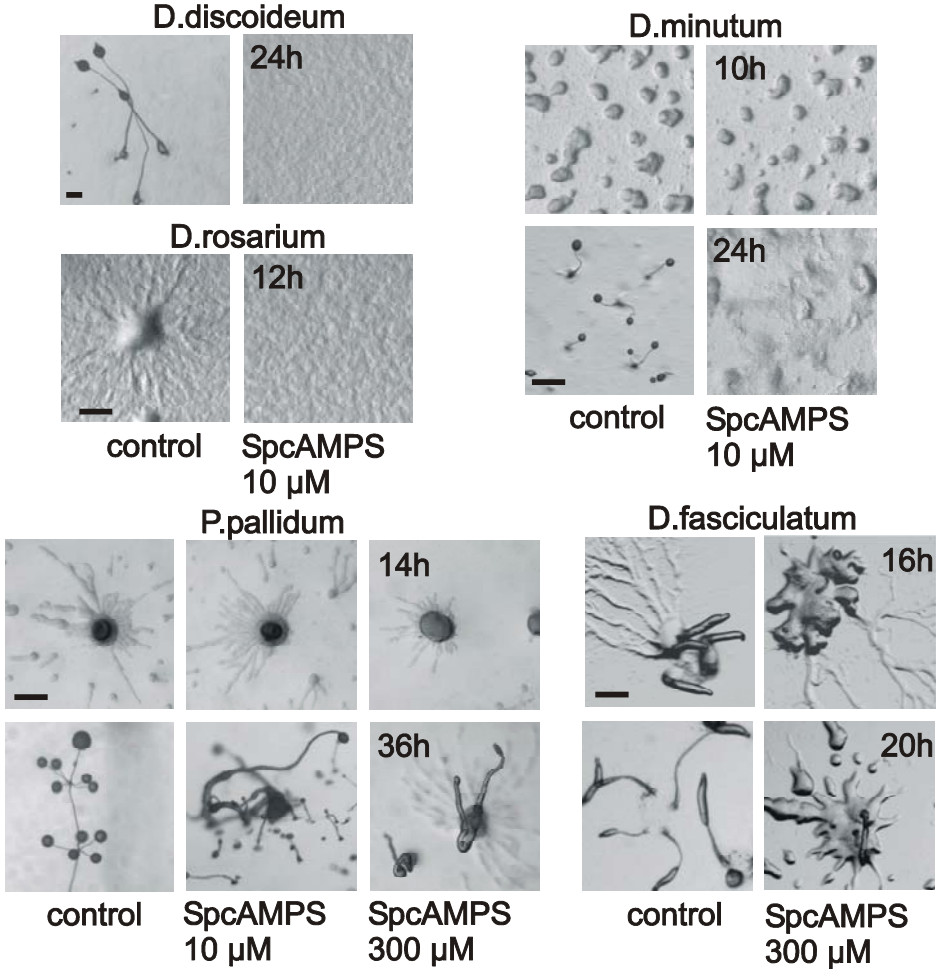

Figure 5. Effects of SpcAMPS on *Dictyostelid* development Cells from the indicated species were distributed at 2 x 10^5 cells per cm^2 on nonnutrient agar (control) or agar with 10 or 300 µM SpcAMPS and incubated at 22°C. The progression of development was photographed at 2-h intervals. Bar, 200 µm.

Conclusions

We identified *DdcAR1* orthologs in species belonging to three taxa, *D.fasciculatum, P.pallidum and D.minutum* that do not use cAMP to aggregate. The cAMP binding properties of the *DmcAR* are similar to those of *DdcAR1*, and *DmcAR* fully restores oscillatory signalling and development in a *D.discoideum car1car3* mutant. *D.minutum, P.pallidum* and *D.fasciculatum* each represent earlier branches off the main line of descent leading to *D.discoideum* (Fig. 1A) (20). In contrast to *D.discoideum,* two of these species express *cAR1* only during fruiting body formation (Fig. 1C). In all three cases only fruiting body formation, and not aggregation, is disrupted when cAR function is blocked (Fig.5) (21). This strongly suggests that coordination of fruiting body morphogenesis is the ancestral function of extracellular cAMP signalling, while its role in *D.discoideum* and *D.rosarium* aggregation is evolutionary derived.

The spiral waves of cell movement that are triggered by cAMP oscillations in a field of starving *D.discoideum* cells are one of the most striking examples of self-organization in biology. We now show that they also represent a stunning example of a derived evolutionary novelty. How might this novel feature have come about? The promoter structure of cAMP sig-

nalling genes in *D. discoideum* suggests a mechanistic explanation for this alteration. The extracellular phosphodiesterase *DdPdsA* gene has three separate promoters for expression during growth, aggregation and fruiting body (late) morphogenesis respectively. The late promoter is proximal to the coding sequence, followed by the growth-specific promoter and finally the aggregation promoter (37). *DdcAR1* has two separate promoters; the late promoter, proximal to the coding sequence, is for expression during fruiting body formation, whereas the aggregation promoter is distal to the late promoter (30). We hypothesize that the proximal promoters direct the ancestral function of the cAMP signalling genes in fruiting body morphogenesis, while the distal promoters were acquired later to accommodate the derived roles of cAMP in early development.

Pathway co-option through the acquisition of novel promoter elements is not the entire story, however, as evidenced by the intermediate species *D. minutum*, which shows altered cAR gene expression but lacks aggregation to cAMP. We show that *DmcAR* encodes a fully functional cAMP receptor, which suggests that aggregation to cAMP has not been lost in *D. minutum*. Rather, we propose that aggregation to cAMP has simply not been fully gained, either because this species lacks other components of the signalling pathway, or because the recruited pathway is not completely coupled to the downstream factors required for activity. The cAMP signalling system in Dictyostelids is composed of at least three major parts: cAMP production by adenylyl cyclases, reception by cARs, and degradation by specific phosphodiesterases. Here just one part of this apparatus is considered, but future work will seek to elucidate the route taken towards this evolutionary novelty by considering each component independently and then together. Through this approach, we hope to begin to understand the origin of new traits via gene recruitment.

Acknowledgement: We thank Jim C. Cavender, Guenther Gerisch and Hiromitsu Hagiwara for their kind gifts of D.fasciculatum SH3, *D.minutum* 71-2, *P.pallidum* TNS-C-98 and *D.rosarium* M45 respectively. We thank Peter Devreotes for the gifts of the PJK1 and A15:DdcAR1 vectors and Robert Insall for the *car1car3* cell line. We are grateful to Dirk Dormann for advice on time-lapse videomicroscopy. This research was supported by BBSRC grant 94/COD16760, Dutch Science Foundation (NWO) grant 805.17.047 and Wellcome Trust Grant 057137.

Genbank accession numbers: DdcAR2: A46390; DdcAR3: A46391; DdcAR4: A54813; DrcARI: AY839643; DrcARII: AY839644; DmcAR: AY518271; DfcAR: AY518272; PpTasA: AB045712; AtGPCR: AAM20722; DdcrlA: AAO62367; NcGPCRα: EAA35706 and NcGPCRβ: EAA28751.

References

1. Long, M., Betran, E., Thornton, K. & Wang, W. (2003) Nat. Rev. Genet. 4, 865–875.
2. True, J. R. & Carroll, S. B. (2002) Annu. Rev. Cell Dev. Biol. 18, 53–80.
3. Lee, P. N., Callaerts, P., de Couet, H. G. & Martindale, M. Q. (2003) Nature 424, 1061–1065.
4. Irish, V. F. (2003) BioEssays 25, 637–646.
5. Raper, K. B. (1984) The Dictyostelids (Princeton Univ. Press, Princeton).
6. Siegert, F. & Weijer, C. J. (1992) Proc. Natl. Acad. Sci. USA 89, 6433–6437.
7. Konijn, T. M., Van De Meene, J. G., Bonner, J. T. & Barkley, D. S. (1967) Proc. Natl. Acad. Sci. USA 58, 152–1154.
8. Pitt, G. S., Milona, N., Borleis, J., Lin, K. C., Reed, R. R. & Devreotes, P. N. (1992) Cell 69, 305–315.
9. Lacombe, M. L., Podgorski, G. J., Franke, J. & Kessin, R. H. (1986) J. Biol. Chem. 261, 16811–16817.
10. Devreotes P. N., Neuron 12, 235-241 (1994).
11. Aubry L., Firtel R., Ann. Rev. Cell. Dev. Biol. 15, 469-517 (1999).
12. Shimomura, O., Suthers, H. L. B. & Bonner, J. T. (1982) Proc. Natl. Acad. Sci. USA 79, 7376–7379.
13. Cocucci, S. & Sussman, M. (1970) J. Cell Biol. 45, 399–407.
14. Don, R. H., Cox, P. T., Wainwright, B. J., Baker, K. & Mattick, J. S. (1991) Nucleic Acids Res. 19, 4008–4008.
15. Sun, B., Ma, H. & Firtel, R. A. (2003) Mol. Biol. Cell 14, 4526–4540.
16. Nellen, W., Datta, S., Reymond, C., Sivertsen, A., Mann, S., Crowley, T. & Firtel, R. A. (1987) in Methods in Cell Biology, ed. Spudich, J. A. (Academic, Orlando, FL), Vol. 28, pp. 67–100.
17. Sambrook, J. & Russell, D. (2001) Molecular Cloning: A Laboratory Manual (Cold Spring Harbor Lab. Press, Plainview, NY).
18. Insall, R. H., Soede, R. D. M., Schaap, P. & Devreotes, P. N. (1994) Mol. Biol. Cell 5, 703–711.
19. Verkerke-VanWijk, I., Kim, J. Y., Brandt, R., Devreotes, P. N. & Schaap, P. (1998) Mol. Cell. Biol. 18, 5744–5749.
20. Siegert, F., and Weijer, C. (1989) J Cell Sci 93, 325-335.
21. Siegert, F., and Weijer, C. J. (1995) Curr Biol 5, 937-943.
22. Thompson, J. D., Gibson, T. J., Plewniak, F., Jeanmougin, F. & Higgins, D. G. (1997) Nucleic Acids Res. 25, 4876–4882.
23. Ronquist, F. & Huelsenbeck, J. P. (2003) Bioinformatics 19, 1572–1574.
24. Felsenstein, J. (2004) PHYLIP Phylogeny Interference Package (Univ. of Washington Seattle), Version 3.6b,
25. Jones, D. T., Taylor, W. R. & Thornton, J. M. (1992) Comput. Appl. Biosci. 8, 275–282.
26. Strimmer, K. & Von Haeseler, A. (1996) Mol. Biol. Evol. 13, 964–969.
27. Schaap, P., Winckler, T., Nelson, M., Alvarez-Curto, E., Elgie, B., Hagiwara, H., Cavender, J., Milano-Curto, A., Rozen, D. E., Dingermann, T., et al. (2006). Science 314, 661-663.
28. Kawabe, Y., Kuwayama, H., Morio, T., Urushihara, H. & Tanaka, Y. (2002) Gene 285, 291–299
29. Saxe, C. L., III, Johnson, R. L., Devreotes, P. N. & Kimmel, A. R. (1991) Genes Dev. 5, 1–8.
30. Louis, J. M., Saxe, C. L., III, & Kimmel, A. R. (1993) Proc. Natl. Acad. Sci. USA 90, 5969–5973.
31. De Wit, R. J. W. & Konijn, T. M. (1983) Cell Differ. 12, 205–210.
32. Henderson, E. J. (1975) J. Biol. Chem. 250, 4730–4736.
33. Van Lookeren Campagne, M. M., Schaap, P. & Van Haastert, P. J. M. (1986) Dev. Biol. 117, 245–251.
34. Tomchik, K. J. & Devreotes, P. N. (1981) Science 212, 443–446.
35. Rossier, C., Gerisch, G., Malchow, D. & Eckstein, F. (1978) J. Cell Sci. 35, 321–338.
36. Van Haastert, P. J. M. & Van der Heijden, P. R. (1983) J. Cell Biol. 96, 347–353.
37. Faure, M., Franke, J., Hall, A. L., Podgorski, G. J. & Kessin, R. H. (1990) Mol. Cell. Biol. 10, 1921–1930.
38. Scatchard, G. (1949) Ann. N.Y. Acad. Sci. 51, 660–672.
39. Klein, P. S., Sun, T. J., Saxe, C. L., III, Kimmel, A. R., Johnson, R. L. & Devreotes, P. N. (1988) Science 241, 1467–1472.